Supplementary Information for

Digital Microfluidic Hemagglutination Assays for Blood Typing, Donor Compatibility Testing, and Hematocrit Analysis

This PDF file includes:

Methods Section
Supplemental Tables
Supplemental Figures
Legends for Supplemental Movies

Other supplementary materials for this manuscript include the following:

Supplemental Movies

Methods

Materials and reagents

Deionized water (DI H_2O) had a resistivity of >18 megaohm·cm at 25°C. Stock surfactant solution was Dulbecco's phosphate buffered saline (DPBS, Sigma-Aldrich) supplemented with 5% (w/v) ethylenediamine tetrakis(ethoxylate-block-propoxylate) tetrol (Tetronic 90R4, BASF Corp.). Blood typing reagent solutions [Seraclone anti-A (801320), Seraclone anti-B (801345), Seraclone anti-AB (801370), Seraclone anti-D Blend (802031) and Seraclone Control AB0 Rh (805171)] were purchased from Bio-Rad Laboratories, supplemented with 0.05% (w/v) Tetronic 90R4, and were used as a liquid solution or were lyophilized on the surfaces of DMF devices. Chemical agglutination agent solution was DPBS supplemented with 1% (w/w) poly(diallyldimethylammonium chloride) (Merquat 100, MW ~240,000, Polysciences) and 0.1% (w/v) Tetronic 90R4.

Blood collection

Blood was collected from three sources for analysis by the new technique. (1) Venipuncture blood samples from healthy donors with known blood type were purchased from Innovative Research, supplied in Vacutainer® K2EDTA tubes (BD) (10 mL). (2) Finger-prick blood samples were collected in Microtainer® K2EDTA tubes from healthy volunteers following Protocol #: 00037583, which was reviewed and approved by the University of Toronto Research Ethics Board (REB). Sixteen of the samples had known blood types (verified via donor-cards or official documentation), while twelve were unknown. In some cases, finger-prick blood samples were centrifuged in a 0.2 mL microcentrifuge tube at 300 g for 5 minutes, and the plasma was recovered to be used as potential donor plasma samples for DMF mock-donor compatibility tests. (3) Adult whole blood samples were collected from the Sunnybrook Transfusion Medicine and Tissue Bank following Protocol #: 1637, which was reviewed and approved by the Sunnybrook Health Sciences Centre REB. These pre-centrifuged blood samples were gently re-suspended on an automated rocker for 2 hours, after which 1 mL aliquots were collected for analysis.

DMF device fabrication and operation

DMF bottom plates (50.8 mm x 76.2 mm x 1.1 mm) bearing electrodes coated with Parylene C and Fluoropel PFC 1104V were fabricated in the University of Toronto Nanofabrication Centre cleanroom facility as described previously (*Lab Chip* 2015, 15:3776–84). The bottom plate design featured an array of 68 square actuation electrodes, 8 rectangular electrodes used for dispensing, and 8 reservoir electrodes. Each electrode was connected via a patterned wire that interfaced with an array of contact pads on the side of the device. DMF top plates consisted of ITO-glass slides (25.4 mm × 50.8 mm × 0.7 mm, Riley Supplies) coated with FluoroPel PFC 1104V as described previously (*Lab Chip* 2016, 16:4560–8). Each device was assembled by joining a top and bottom plate with two pieces of double-sided tape (Scotch Permanent Double Sided Tape, 3M), which served as a spacer, creating an inter-plate gap of approximately 200 µm. Unit droplets (i.e., those that covered a single actuation electrode) were approximately 920 nL, and reservoir volumes (i.e., droplets that covered a single reservoir electrode) were approximately 6 µL. Devices were managed using a customized, lab-built version of the open-source DropBot system (*Appl. Phys. Lett.* 2013, 102:193513), version 3.0, https://github.com/sci-bots/dropbot-v3, that includes the capacity to interface with a peripheral board to control a micro-pump (described below), and to operate for up to 12 h on battery power. The DropBot and micro-pump were controlled using a custom version of MicroDrop software (version 2.31.1). Devices were interfaced to the DropBot and were actuated by applying 100 V_{RMS} square waves at 10 kHz (parameters determined to generate forces below velocity-saturation (*Langmuir* 2019, 35:5342–52) for the liquids used here) in pre-programmed steps to facilitate droplet dispensing, moving, and mixing.

Pump and operation

The custom version of DropBot used here included an integrated mp6 Piezoelectric Diaphragm Micropump (Servoflo Corp.). The pump was connected to a 14 cm long section of 1.3 mm i.d., 3.0 mm o.d. Tygon® tubing (mp-t, Servoflo Corp.) interfaced on one side to a microcentrifuge tube (pump reservoir), and the other side to a 10 µL pipette tip, cut to 5 mm total length (from the narrow side), that was positioned at the interface of the DMF top and bottom plate in a DMF reservoir. A passive check valve (mp-cv, Servoflo Corp.) was integrated between the

pump and the pipette tip to minimize backflow. The DropBot featured a peripheral custom microcontroller board based on ATMEGA328 (Microchip Technology Inc.) that drove the mp6-OEM controller (Servoflow Corp.), which controlled the pump operation (pump status and flow rate). Briefly, the pump was actuated by applying square wave pulses (270 V_{pp}) at varying frequencies (0.0625 Hz – 625 Hz) to control the flowrate (6 µL/min – 3.7 mL/min), calibrated by measuring the mass of fluid pumped as a function of time. Centralized control from DropBot enabled synchronization between the pump dispensing and the DMF electrode-state. In typical experiments, the pump was used to deliver reconstitution solvent [DI H_2O supplemented with 0.05% (w/v) Tetronic 90R4] to the DMF device at 3.6 mL/min (100 Hz frequency) in purge mode (during priming of the pump prior to experiments or purging solvent at the end of experiments), and 220 µL/min (500 Hz frequency) in dispense mode (during experiments: filling/refilling of a DMF reservoir).

A six-step closed-loop automated protocol was developed to automatically fill and refill designated DMF reservoirs with reconstitution solvent. In step 1, the capacitance of the empty reservoir electrode was recorded to define the background capacitance. In step 2, the pump was engaged to dispense a series of discrete volumes (each ~500 nL) onto the reservoir electrode. After each dispense step, the capacitance was measured, and after the third step, a line was fitted to the first three capacitance measurements. Dispense-and-measure steps were continued until the capacitance deviated 90% from the value predicted by the line fitted in step two. This capacitance value was recorded as the 'threshold.' In step 3, two additional ~500 nL volumes were then dispensed to cause the reservoir to be slightly 'over-filled,' at which point the device was ready for digital microfluidic operations (steps 4 and 5). When appropriate for an experiment, a single-unit droplet (step 4) or a double-unit droplet (step 5) was dispensed onto the array of driving electrodes. In step 6, the pump was engaged again to dispense a series of ~500 nL volumes onto the reservoir until it was 'over-filled' (see step 3 for details) and was ready for additional operations.

The pump was used with DMF devices that were modified with dried reagents prior to use. Briefly, the top plate of an assembled device was removed, and 1 µL aliquots of blood typing antibody solutions and/or 2 µL aliquot(s) of chemical agglutination solution were deposited on designated actuation electrode(s) on the bottom plate. The top plate was replaced, and the device was frozen at -80 °C for 10 minutes, and lyophilized (Labconco Freeze Dryer) over-night at ~0.005 mm Hg, and then stored at room temperature until use. In reconstitution experiments, reconstitution solvent was loaded onto the device manually or via the integrated pump (as above), and one or more single-unit droplets (one for each reagent) were dispensed onto the array, driven onto the lyophilized reagent-spot(s), and actuated between neighboring electrodes for ~5 seconds to reconstitute the dried reagent(s) and form solution(s) to be used for analysis (as below).

DMF blood typing, donor compatibility, and hematocrit analysis

All steps required for the assays were pre-programmed in a protocol on the MicroDrop software. A custom graphic user interface was written in Python to interface with MicroDrop, to control the processes of capturing images, running the image analysis algorithm, collecting sample-related information (such as patient ID), and returning the result in a digital patient card format. In many experiments, solution-phase reagents were used to implement a four-step assay procedure. In step 1, reagent solution(s) were loaded into reservoirs and droplet(s) were dispensed onto the array of actuation electrodes. In step 2, a blood sample was loaded into a reservoir and droplet(s) were dispensed onto the array. In step 3, blood- and reagent-droplet pair(s) were merged and actively mixed (by repeatedly translating each merged droplet in a circular pattern at ~1.5 mm/s around the eight electrodes adjacent to the original position of the reagent-droplet), and in step 4, the results were characterized. Operational and methodological details for each assay are given in Supplemental Table 2. In other experiments (implemented with devices bearing dried reagents), step 1 was replaced with the solvent dispensing and reagent-dissolution procedure described above.

Droplet Agglutination Assessment on Digital Microfluidics (DAAD)

The DAAD algorithm was written and applied in Python using the OpenCV library (G. Bradski, *The OpenCV Library*. Dr. Dobb's Journal of Software Tools, 2000) in eight sub-steps. The first six sub-steps (i – vi) were the same for blood typing/donor testing and hematocrit analysis: (i) One of two cameras (which were separately integrated into the DropBot at different times) was used to collect an image of the device: the USB8MP02G-L75-CA (ELP, Amazon.ca) or the C525 (Logitech, Amazon.ca). Each camera was positioned at a 40-degree angle relative to the plane perpendicular to the DMF device and at a distance at least 5 cm away from the device. Images were typically captured at the maximum resolution of each camera (3264×2448 pixels for the ELP, 1600×896 pixels for the Logitech). (ii) The image was transferred to the laptop computer over USB and then was corrected for perspective by defining four coordinates in the source image and four reference coordinates. A 3×3 matrix was calculated based on each set of coordinates (image – reference corresponding pair) and then the same matrix was applied to the source image to acquire the perspective-corrected image. (iii) The center of the DMF device in the corrected image was located automatically by detecting known device features, and this region of the image was isolated for further processing. (iv) The droplets were detected by identifying contours and combining neighboring contours to form a region of interest (ROI) for each droplet which was used to define a mask to extract an image. (v) The ROI image corresponding to each droplet was masked, isolated and converted from RGB to grayscale. (vi) Each isolated image was flattened into a one-dimensional array and normalized such that the pixel intensities covered the full 8-bit range [0-255], and then sorted by pixel-value from lowest to highest.

In blood typing (b) and donor compatibility testing (d) experiments, DAAD sub-steps (i-vi) were followed by DAAD sub-steps (vii-bd) and (viii-bd). (vii-bd) A line was drawn between the pixel intensities found at 42% and 84% of the total number of pixels (boundaries determined empirically to give the best performance), and the slope of the line was defined as the 'agglutination score'. [In initial experiments, a calibration set of ROI images collected from 25 whole blood samples (4 antibodies, 100 droplets) were evaluated to define the 'agglutination threshold' of 0.1512 a.u.] Each droplet's agglutination score was compared to the threshold to determine positive vs. negative. (viii-bd) A digital patient card was returned to the user featuring RGB images of the four droplets, as well as a summary-determination of blood type or donor compatibility.

In hematocrit analysis (h) experiments, DAAD sub-steps (i-vi) were followed by DAAD sub-steps (vii-h) and (viii-h). (vii-h) The integral of the pixel intensities found (inclusively) between 15% and 85% of the total number of pixels (boundaries determined empirically to give best performance) was defined as the 'hematocrit score'. (In initial experiments, hematocrit scores from a calibration set of diluted blood samples with artificially defined hematocrit levels between 20 and 60% were found and plotted as a function of hematocrit level and fitted with a second order polynomial: $y = -0.0249x^2 + 1.092x + 107.3$.) Each droplet's hematocrit score was compared to the calibration plot to determine the predicted % hematocrit. (viii-h) A digital patient card was returned to the user featuring an image of the droplet with the estimated % hematocrit.

In some blood-typing experiments, three alternative agglutination detection algorithms were tested and compared to DAAD: the histogram method, the standard deviation method and the variance method. In the histogram method, DAAD sub-steps (i) – (v) were performed to isolate each ROI image. For each image, a histogram was generated from the number of pixels for each pixel intensity value. The histogram was smoothed with a moving average filter (window = 10 bins), and in the smoothed dataset, the major peaks were identified by finding local maxima by comparison of pixel intensities with neighboring values. The average pixel intensity of the major peaks in the smoothed histogram was defined as the threshold T. Finally, the agglutination score was defined as $100\times(S_{>T}/S)$, where S is the number of pixels in the ROI image and $S_{>T}$ is the number of pixels with intensity greater than T. In the standard deviation method [adapted from a previous report (*Genes* 2018, 9:281). DAAD sub-steps (i) – (vi) were performed, after which the array was normalized (again) to the range [0,1], and the standard deviation σ of pixel intensities was defined as the agglutination score. In the variance method, adapted from previous reports (*Biosens. Bioelectr.* 2017, 93:110–7; *High-Throughput* 2018, 7:10; *Anal. Chem.* 2008 80:6190–7).

DAAD sub-steps (i) – (v) were performed to isolate each ROI image. The local variance of each pixel intensity relative to those of its adjacent neighbors σ_p^2 was calculated using a 3×3 matrix, and the average variance of all of the pixel intensities in the image $\overline{\sigma_p^2}$ was determined. The agglutination score was defined as $100\times\overline{\sigma_p^2}$. The calibration set of 100 ROI images (from 25 whole blood samples) that was used to define the agglutination score threshold for DAAD was used for the same purpose for the alternate methods, and the best agglutination thresholds were found to be 6.629 a.u., 0.131 a.u., and 5.528 a.u., for the histogram method, standard deviation method, and the variance method, respectively.

DAAD for Blood Type Scoring

In some experiments, DAAD blood type analysis was extended from predicting binary results (positive vs. negative) to predicting the degree of agglutination. In these experiments, DAAD sub-steps (i-v) were followed by image binarization using thresholding and denoising of the binarized image with morphological open and close transformations to generate a processed binary image. Then, contours were traced in the processed binary image and used to generate a feature vector of size 15, where each element in the vector was a value representing a feature in the ROI image (Supplemental Table 6).

A dataset of 567 ROI images was annotated manually by two annotators, who assigned an integer agglutination score label from 0 to +4 (*ISBT Science Series*. 2008, 3:33-60). The few cases with disagreement by the annotators were reviewed and reconciled. The dataset was evaluated by six machine learning regression models (linear regression, stochastic gradient descent, multilayer perceptrons, AdaBoost, random forests, and gradient boosting trees) from the Scikit-learn Python package *(J. Machine Learning Res.* 2011. 12:2825-2830). Regression outputs were rounded to the nearest 0 to +4 integer and model accuracy was computed against the assigned (integer) labels. A ten-fold cross-validation procedure was applied in which the 567 images were divided into 10 partitions (folds), where 9 folds were used as training data (to tune model hyperparameters) to generate a unique model for the 10th, iterating through to generate a model for each fold in the set. The final model accuracy was defined as the average accuracy across all data-samples. The average accuracies for each regression model are presented in Supplemental Table 7. The best performing model was gradient boosting trees; Supplemental Fig. 8 illustrates the predicted results versus the assigned labels.

Non-DMF blood typing and hematocrit analysis

For manual blood-typing in tubes, each whole blood sample to be analyzed was diluted to 5% in DPBS. Four 20 µL aliquots of this solution were prepared, and each was combined with a 20 µL aliquot of one of the blood typing antibody solutions, which was gently mixed by flicking the tube 5 times. Each mixture was centrifuged at 1000 g (Micromax, Thermo) for 20 s, after which the tube was gently shaken to dislodge the RBC pellet, by repeatedly and gently flicking the tube up to 10 times. Each tube was visually observed and determined to be positive in cases in which the pellet or large parts of the pellet did not resuspend.

For manual blood-typing using ELDON™ cards, ELDON™ Home Kits HKA 2511 were purchased from Amazon.ca and used as per their instructions. Briefly, tap water droplets were dispensed onto the cards to solubilize dried reagents with the dropper included with the kit. A pin-prick of blood was formed, and spatulas included with the kit were used to collect aliquots of blood and to smear them onto the solubilized reagents for 10 s each. The card was then tilted and rocked for 40 seconds. ABO results were available after the 40 second incubation, while the RhD result developed over the course of 2 to 3 minutes. Finally, the results were interpreted by eye according to the instructions and recorded on card. The entire process takes approximately 5 to 10 minutes.

For automated blood-typing, anticoagulated blood samples were manually centrifuged to separate RBCs from plasma and then loaded onto the ORTHO VISION® Analyzer; the remaining steps were performed automatically. (1) A 4% suspension of RBCs was formed in MTS™ Diluent 2 Plus. (2) 10 µL aliquots of the 4% suspension were dispensed into the Anti-A, Anti-B, Anti-D and Control wells of an ORTHO ID-MTS™ A/B/D Monoclonal and Reverse Grouping Card [which

contains wells pre-filled with a dextran acrylamide gel mixed with either Anti-A, Anti-B, Anti-D or control antibodies, and can be used to simultaneously perform forward and reverse grouping analysis]. (3) 50 µL aliquots of 0.8% suspensions of AFFIRMAGEN™ reagent A1 and B red blood cells and 50 µL of plasma were dispensed to the reverse grouping wells of the card. (4) The card was centrifuged at the preset conditions (1014 RPM) according to the manufacturer's guidelines, and then (5) removed from the centrifuge and automatically observed for agglutination assessment. This process takes approximately 30 minutes.

For manual hematocrit testing (microhematocrit), in each analysis a 75 mm hematocrit tube (Heparinized Hemato-Clad®, Drummond) was filled with whole blood to approximately 75% of the total volume of the tube. Next, a small piece of Play-Doh compound was used to seal the bottom end of the tube, and a batch of tubes to be evaluated was inserted into a piece of Styrofoam (to stabilize the tubes) positioned in the bottom of a 50 mL falcon tube, and centrifuged at 300 g (ST 40R, Thermo) for 10 min. The hematocrit of each sample was then assessed using a capillary reading card (Critocaps micro-hematocrit tube reader, Thomas Scientific). In comparisons to DAAD analyses, Prism 7 by GraphPad was used to perform a Bland-Altman analysis.

Supplemental Table 1. Comprehensive list of previous publications describing microfluidic blood typing (shaded grey), donor matching, or hematocrit measurement techniques.

	Reference	Type†	Class‡
1	Chen et al. *Biomicrofluidics.* 2019. 13:34107.	B	L, M
2	Chang et al. *Biosensors and Bioelectronics.* 2018. 102:234–41.	B	L
3	Huet et al. *Biosensors and Bioelectronics.* 2017. 93:110–7.	B	L, M
4	Huet et al. *High-Throughput.* 2018. 7:10.	B	L, M
5	Lee et al. *Sensors and Materials.* 2005. 17:113–23.	B	L, M
6	Kline et al. *Analytical Chemistry.* 2008. 80:6190–7.	B	L, M
7	Li et al. *The Analyst.* 2013. 138:4933.	B	L, M
8	Makulska et al. *Lab on a Chip.* 2013. 13:2796–801.	B	L
9	Su et al. *Cellulose.* 2012;19. 1749–58.	B	L
10	Zhang et al. *Science Translational Medicine.* 2017. 9:eaaf9209.	B	L
11	Kang et al. *Journal of Manufacturing Science and Engineering*. 2004. 126:766–71.	B	L, M
12	Pipatpanukul et al. *Vox Sanguinis.* 2016. 110:60–9.	B	L, M
13	Srivastava et al. *Electrophoresis.* 2011. 32:2530–40.	B	L, M
14	Li et al. *Sensors and Actuators B: Chemical.* 2018. 262:411–7.	B	L, M
15	Hertaeg et al. *The Analyst.* 2021. 146:1048–56.	B	L, M
16	Nilghaz Aet al. *Analytical and Bioanalytical Chemistry.* 2016. 408:1365–71.	B	L, M
17	Then et al. *Scientific Reports.* 2017. 7:1616.	B	L, M
18	Chang et al. *SLAS Technology.* 2018. 23:172–8.	B	L, M
19	El Kenz & Corazza. *Vox Sanguinis.* 2015. 109:79–85.	B	L
20	Choi et al. *Microsystem Technologies.* 2009. 15:309–16.	B	Q
21	Al-Tamimi et al. *Analytical Chemistry.* 2012. 84:1661–8.	B	Q
22	Li et al. *Angewandte Chemie - International Edition.* 2012. 51:5497–501.	B	Q
23	Khan et al. *Analytical Chemistry.* 2010. 82:4158–64.	B	Q, M
24	Noiphung et al. *Biosensors and Bioelectronics.* 2015. 67:485–9.	B	Q, M
25	Kim et al. *Lab on a Chip.* 2006. 6:794–802.	B	Q, M
26	Park & Park. *Analytical Chemistry.* 2019. 91:11636–42.	B	Q
27	Lin et al. *ACS Sensors.* 2020. 5:3082–3090.	B	Q
28	Yamamoto et al. *Biomicrofluidics.* 2020. 14:24111.	B	Q
29	Karimi et al. *Lab on a Chip.* 2019. 10:24110.	B	Q
30	Songjaroen et al. *Journal of Immunoassay and Immunochem.* 2018. 39:292–307.	B	Q
31	Ansari et al. *Australian Journal of Forensic Sciences.* 2020. 1–12.	B	Q, M
32	Chen et al. *Lab on a Chip.* 2015. 15:4533–41.	B	Q
33	Prathapan Ret al. *ACS Applied Bio Materials.* 2018. 1:728–37.	B	Q, M
34	Ballerini et al. *Analytical and Bioanalytical Chemistry.* 2011;399:1869–75.	B	Q
35	Nilghaz et al. *ACS Applied Materials & Interfaces.* 2014. 6:22209–15.	B	Q
36	Casals-Terré et al. *J. Biomed. Mater. Research B: Appl. Biomater.* 2020. 108:439–50.	B	Q, M
37	Chang et al. *SLAS Technology.* 2019. 24:188–95.	B	Q, M
38	Guan et al. *Analytical Chemistry.* 2014. 86:11362–7.	B	M
39	Ashiba et al. *Sensing and Bio-Sensing Research.* 2015. 3:59–64.	B	M
40	Ashiba et al. *Sensing and Bio-Sensing Research.* 2016. 7:121–6.	B	M
41	Chen et al. *Biomedical Optics Express.* 2018. 9:4604.	B	M
42	Fernandes et al. *IEEE Transactions on Instrument. and Meas.* 2015. 64:112–9.	B, D	M
43	Lee et al. *Electrophoresis.* 2015. 36:978–85.	H	L, Q
44	Kang. *Micromachines.* 2018. 9:475.	H	L
45	Park & Park. *Lab on a Chip.* 2018. 18:1215–22.	D	L
46	Berry et al. *Lab on a Chip.* 2016. 16:3689–94.	H	Q
47	Thompson et al. *Analytica Chimica Acta.* 2016. 924:1–8.	H	

† Type: B = blood typing; D = Donor matching; H = hematocrit measurement
‡ Class: L = large, unintegrated detector; Q = qualitative assessment by "eye"; M = manual intervention req.

Supplemental Table 2. Digital microfluidic assay parameters; all reagents and samples contained 0.1% (w/v) Tetronic 90R4 unless otherwise indicated.

	Blood Typing	Donor Compatibility Testing	Hematocrit Analysis
Step 1	Four[$] antibody solutions (anti-A, anti-B, anti-A,B, and anti-D) loaded into reservoirs, **four single-unit droplets** dispensed	Four-to-five donor plasma[%] samples loaded into reservoirs, **four-to-five single-unit droplets** dispensed	Chemical agglutinating reagent loaded into a reservoir, **one double-unit-droplet** dispensed
Step 2	Whole blood loaded into a reservoir, **four[$] single-unit droplets** dispensed	Whole blood[%] loaded into a reservoir, **four-to-five single-unit droplets** dispensed	Whole blood loaded into a reservoir, **one single-unit droplet** dispensed
Step 3	Reagent droplet-blood droplet pairs actively mixed for **2 min**	Reagent droplet-blood droplet pairs actively mixed for **5 min**	Reagent droplet-blood droplet pair actively mixed for **3 min**
Step 4	Evaluated by eye or camera/DAAD	Evaluated by eye or camera/DAAD	Evaluated by eye or camera/DAAD

[$] In some experiments, an additional solution containing negative ABO & Rh control reagent was loaded, a droplet was dispensed, and mixed with an additional blood unit droplet to serve as a negative control for the assay.

[%] In some experiments, the reagents were reversed, in which whole blood samples were loaded in step 1, and a single plasma sample was loaded in step 2.

Supplemental Table 3. Blood typing results for 12 pin-prick blood samples collected from volunteers at the University of Toronto (part of the validation set) evaluated by DMF-DAAD (column 2) and the conventional manual/tube method (columns 3-4).

	Blood Type		
Sample	**DMF-DAAD**	**Manual/Tube***	
1	A +	A +	A +
2	A +	A +	A +
3	B +	B +	B +
4	B +	B +	B +
5	B +	B +	B +
6	A +	A +	A +
7	A +	A +	A +
8	AB +	AB +	AB +
9	O –	O –	O –
10	A +	A +	A +
11	A +	A +	A –
12	A +	A +	A +

* Manual testing was performed twice, by two different operators. The shaded box indicates that there was a discrepancy between the manual test results for sample 11. In this case, a third manual test was performed by a third operator, which confirmed the type to be A+.

Supplemental Table 4. Blood typing results of 24 blood samples from the Sunnybrook blood bank evaluated by DMF-DAAD (column 2) and the ORTHO VISION® Analyzer (column 3).

	Blood Type		
Sample	**DMF Eye§**	**DMF-DAAD§**	**ORTHO VISION®**
1	A +	A +	A +
2	A +	A +	A +
3	A +	A +	A +
4	A –	A –	A –
5	A –	A –	A –
6	A –	A –	A –
7	B +	B +	B +
8	B +	B +	B +
9	B +	B +	B +
10	B –	B –	B –
11	B –	B –	B –
12	B –	B –	B –
13	O +	O +	O +
14	O +	O +	O +
15	O +	O +	O +
16	O –	O –	O –
17	O –	O –	O –
18	O –	O –	O –
19	AB +	AB +	AB +
20	AB +	AB +	AB +
21	AB +	AB +	AB +
22	AB –	AB –	AB –
23	AB –	AB –	AB –
24	AB –	AB –	AB –

§ DMF assays were run by an operator with no previous experience with microfluidics.

Supplemental Table 5. Representative blood-typing results for samples evaluated by the ORTHO VISION® Analyzer (column 2), DMF-DAAD (column 3), and the ELDON™ card (column 4).

Blood type	ORTHO VISION® ¶	DMF-DAAD ‖	ELDON™ card &
A +	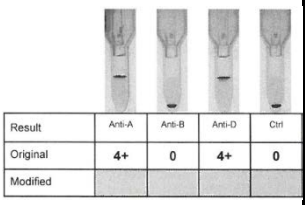	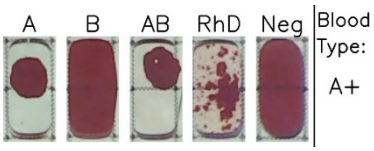	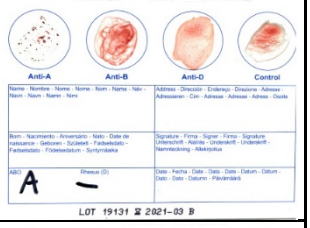
A +	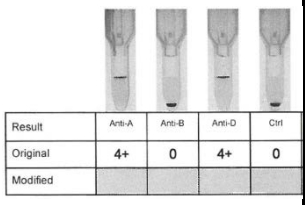	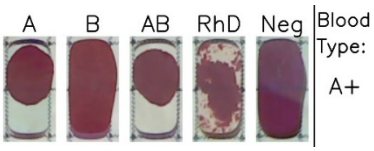	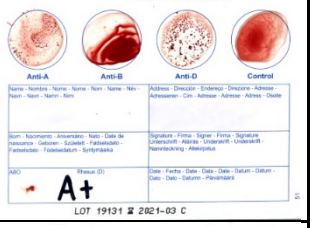
B +	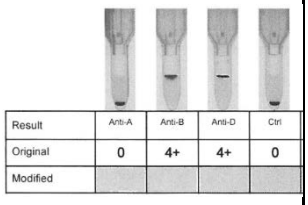	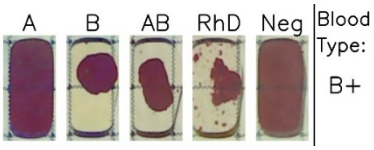	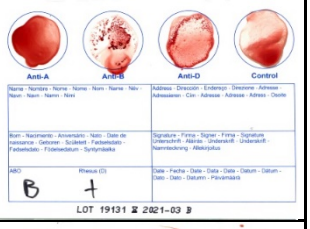
B +	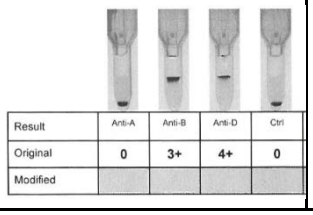	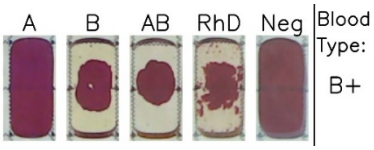	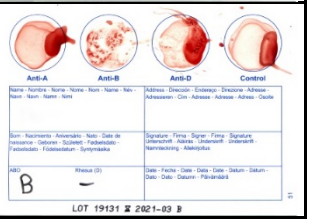

¶ Column 2: ORTHO VISION® Analyzer results from four representative samples (top: two type A+ samples, bottom: two type B+ samples) selected from the set of 24 samples that were analyzed from the Sunnybrook blood bank.

‖ Column 3: DMF-DAAD digital patient information cards from the same samples referenced in column 2.

& Column 4: Pictures of ELDON™ cards used to evaluate four pin-prick blood samples collected from volunteers (top: two type A+ samples, bottom: two type B+ samples). As illustrated, results can be ambiguous, which can lead users to mis-identify the types (as in the Anti-D results in rows 2 and 5).

Supplemental Table 6. Table of feature vectors used as inputs for machine learning models for quantitative agglutination scoring in blood typing experiments.

Element	Feature
1	DAAD binary agglutination score
2	Total pixel area of all contours (foreground)
3	Pixel area of largest contour
4	Total perimeter of all contours
5	Perimeter of largest contour
6	Mean pixel intensity of pixels within all contours
7	Standard deviation of the pixel intensity of pixels within all contours
8	Relative standard deviation of the pixel intensity of pixels within all contours
9	Mean pixel intensity of pixels within the largest contour
10	Standard deviation of the pixel intensity of pixels within the largest contour
11	Relative standard deviation of the pixel intensity of pixels within the largest contour
12	Mean pixel intensity of background pixels
13	Standard deviation of the pixel intensity of background pixels
14	Relative standard deviation of the pixel intensity of background pixels
15	Number of contours detected

Supplemental Table 7. Table of average accuracies for the regression models evaluated for quantitative agglutination scoring in blood typing experiments.

Model	**Accuracy**
Linear Regression	92%
Stochastic Gradient Descent	51%
Multilayer Perceptrons	71%
AdaBoost	96%
Random Forests	96%
Gradient Boosting Trees	**97%**

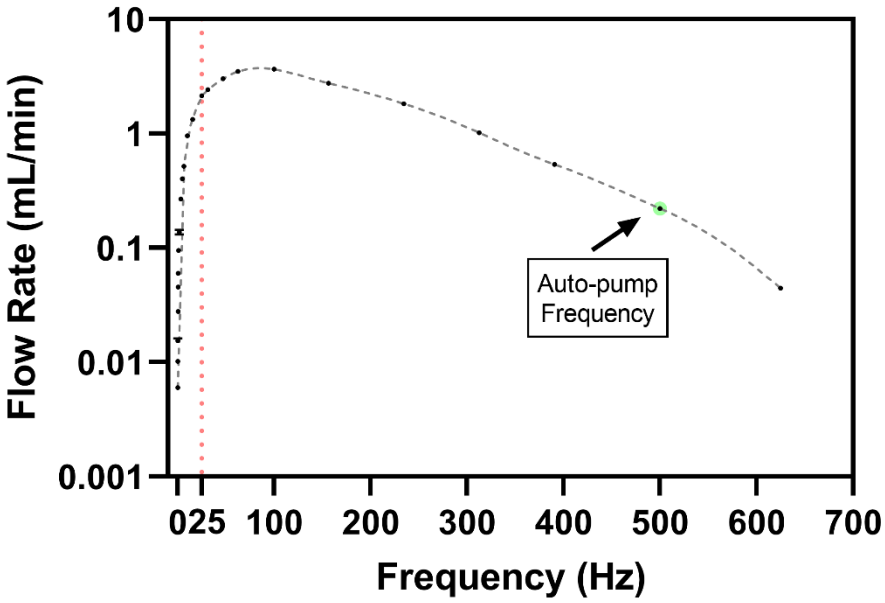

Supplemental Fig. 1. Micropump calibration.
Plot of flow rate of reconstitution solvent as a function of driving frequency for the mp6 piezoelectric diaphragm micropump (Servoflo Corp.) driven by 270 Vpp square waves. The markers are experimental data; the dashed curve was added to guide the eye. Error bars represent ±1 std. dev. from n = 3 replicates. Frequencies below 25 Hz (red dashed line) can be used but the dispense-volumes are unreliable for sub-minute timescales. The frequency of the pump was set at 500 Hz (green highlight, flow rate 220 µL/min) for automated filling and refilling of DMF reservoirs.

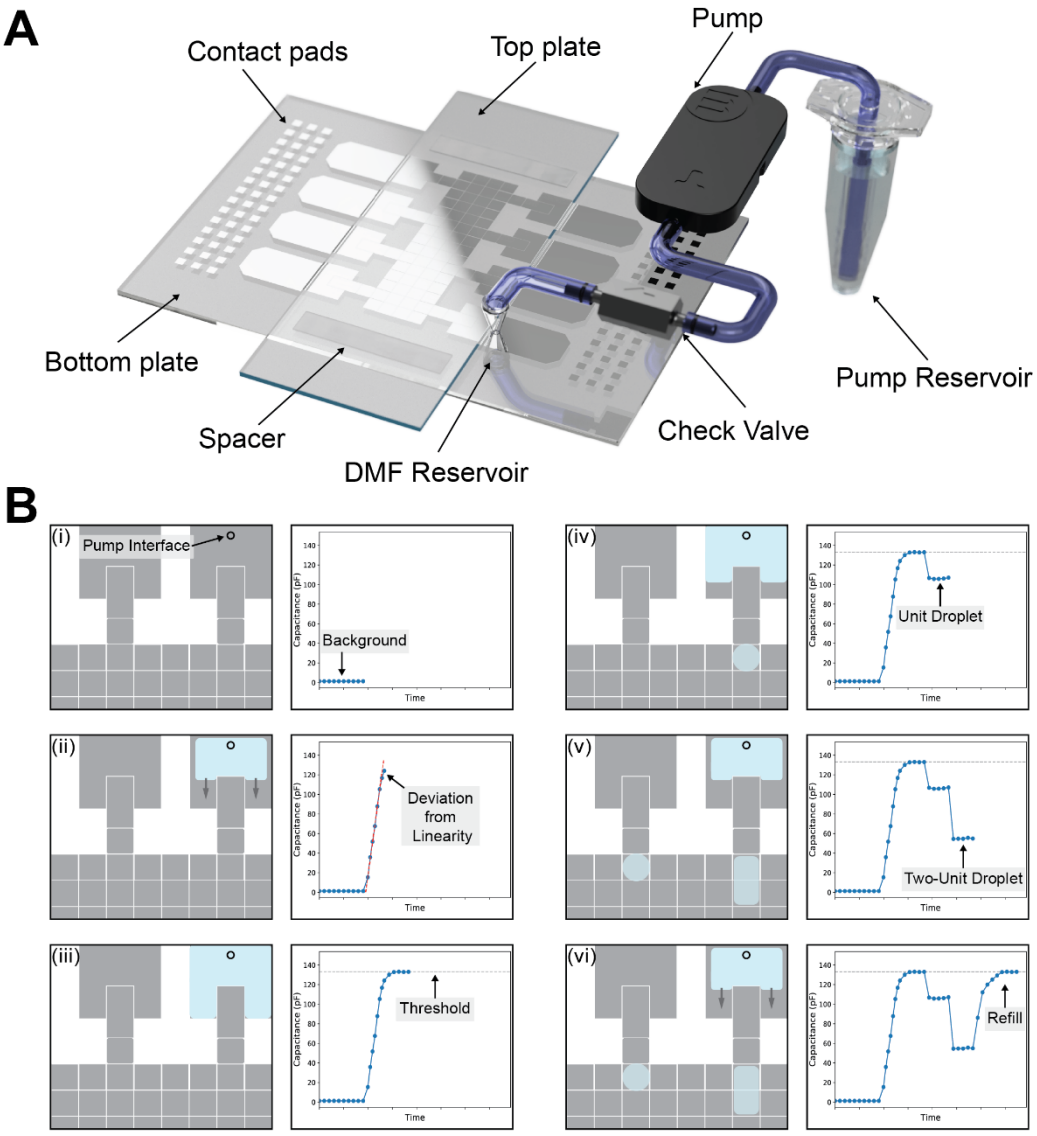

Supplemental Fig. 2. Automatic DMF reservoir refill using the mp6 micro-pump.
(A) Rendered image of a DMF device connected to a micropump (which is integrated into the system shown in Figure 1 in the main text) for the delivery of solvent for the reconstitution of lyophilized reagents. (B) Cartoons (left columns) and corresponding DropBot capacitance readings (right columns) illustrating the operation of the automated reservoir refill on DMF using the integrated mp6 micro-pump. (i) The background capacitance of the empty reservoir is determined by recording multiple measurements and averaging them (n=10). (ii) Calibration: solvent is loaded into the reservoir of the DMF device from the micro-pump in ~500 nL aliquots, measuring the capacitance of the reservoir after each is complete. A line is fitted through the first three capacitance measurements and a threshold is set when a capacitance reading is found to deviate from the line by 10%. (iii) The pump dispenses two more ~500 nL aliquots and the reservoir is defined as being 'over-filled' and ready for use with digital microfluidics. (iv) Dispensing single unit droplets: a single-unit droplet is dispensed onto the array, reducing the volume of liquid in the reservoir, which is reflected in the measured capacitance of the reservoir. (v) Dispensing double unit droplet: Similar to iv, a double-unit droplet can be dispensed, and because the dispensed volume is larger, a larger drop is observed in the measured capacitance of the reservoir. (vi) Reservoir automatic refill: When needed, the micro-pump refills the reservoir to the threshold defined at iii, to indicate that the reservoir is full again.

A

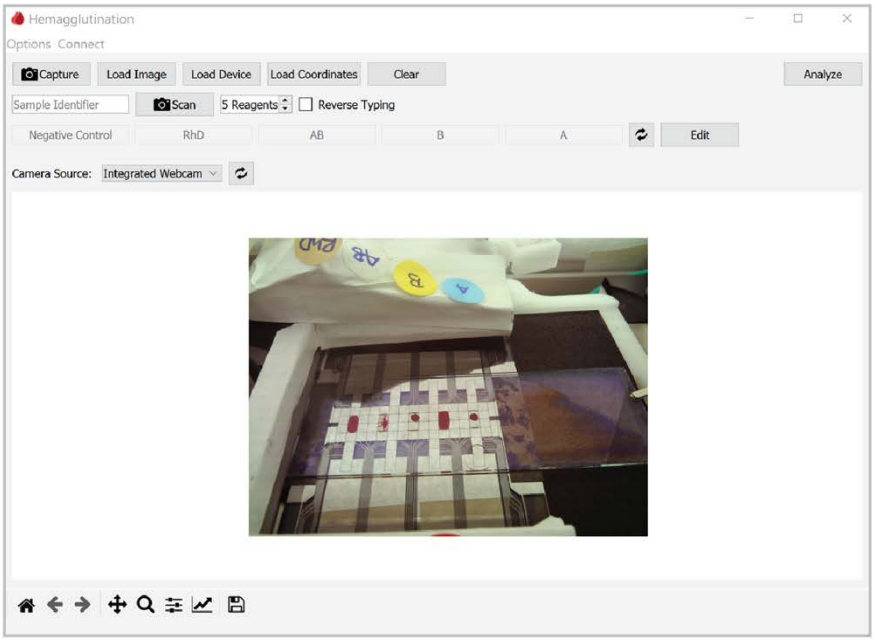

B

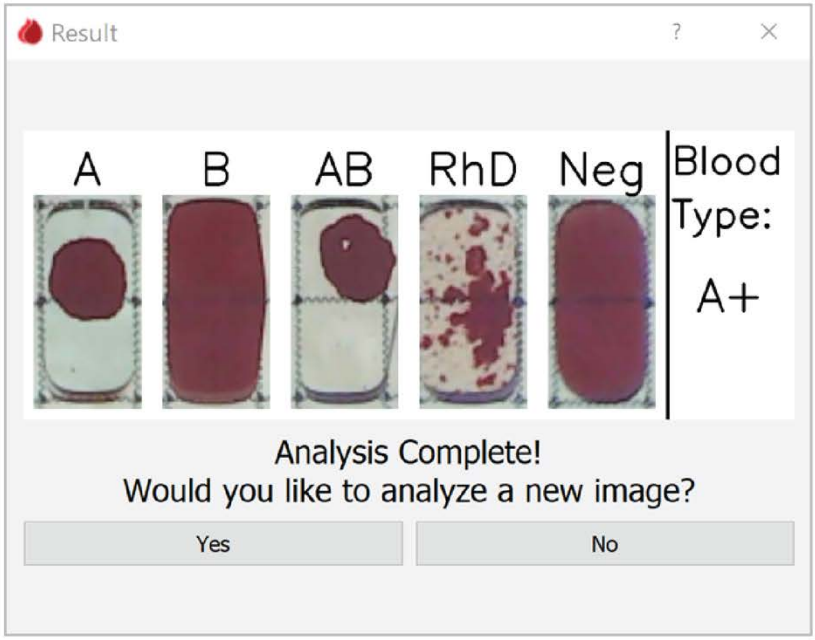

Supplemental Fig. 3. DMF Hemagglutination user interface.
(A) Screenshot of the graphic user interface (GUI) for the new technique. In standard operation, a single click results in the generation of a popup window on the laptop screen (B) featuring a "digital patient card" with the results (in this case, for a representative A+ blood sample). Other options allow the user to input sample information, and to select the desired combination of assays: blood type, donor plasma cross-match, and/or hematocrit analysis

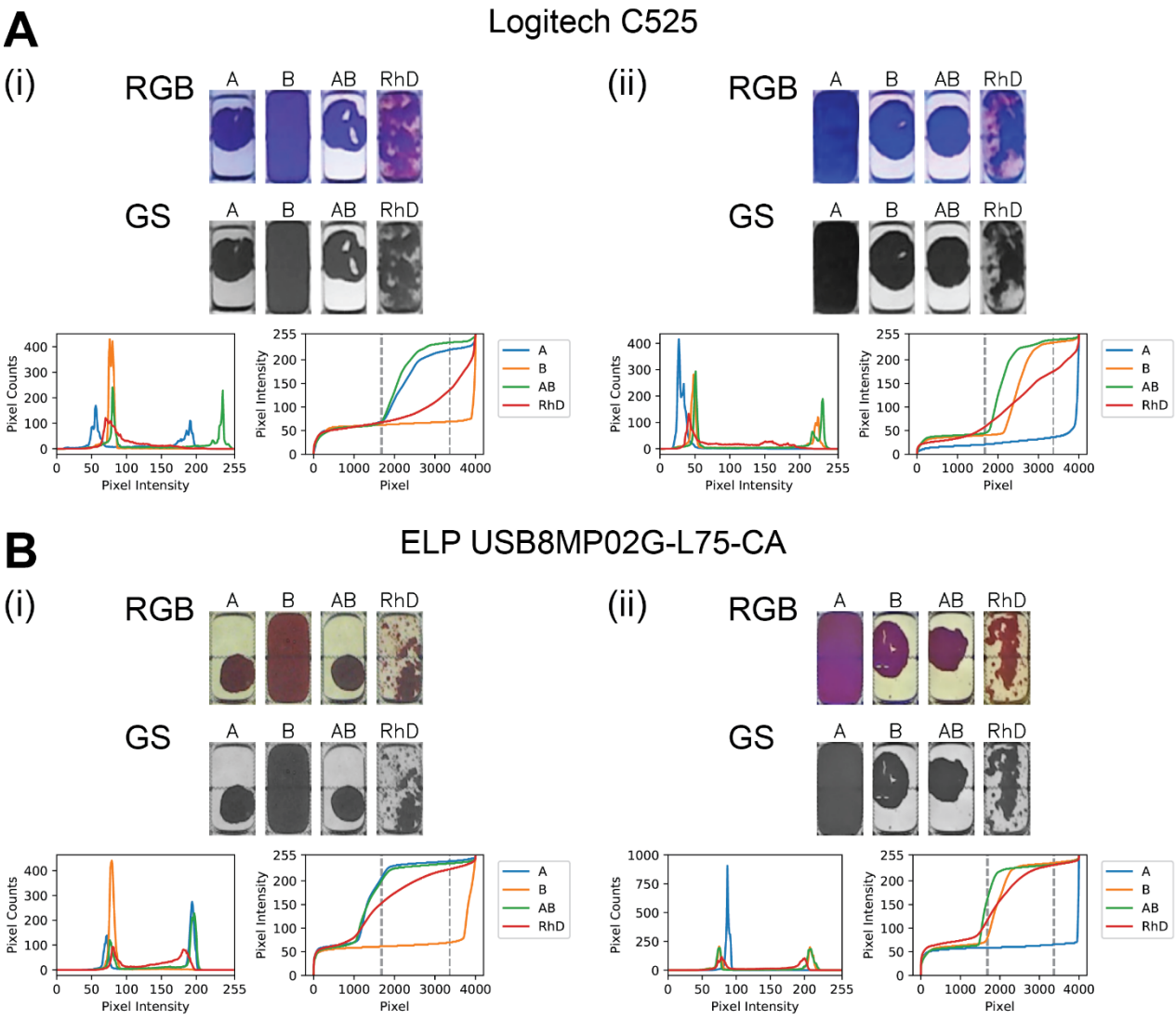

Supplemental Fig. 4. DAAD analysis of blood type with different cameras and imaging conditions.
(A) DAAD analysis with the Logitech C525 camera of (i) a type A+ blood sample with medium brightness, and (ii) a type B+ blood sample with incorrect white balance. (B) DAAD analysis with the ELP USB8MP02G-L75-CA of (i) a type A+ blood sample under low contrast, and (ii) a type B+ blood sample under high contrast. Each sub-panel includes isolated droplet images in RGB (color, top) and GS (grayscale, middle) mode, a histogram correlating to each GS image (bottom left) and a DAAD analysis plot (bottom right). In the graphs, the blue, orange, green, and red line-colors correspond to the droplet with anti-A, anti-B, anti-A,B and anti-D droplets, respectively.

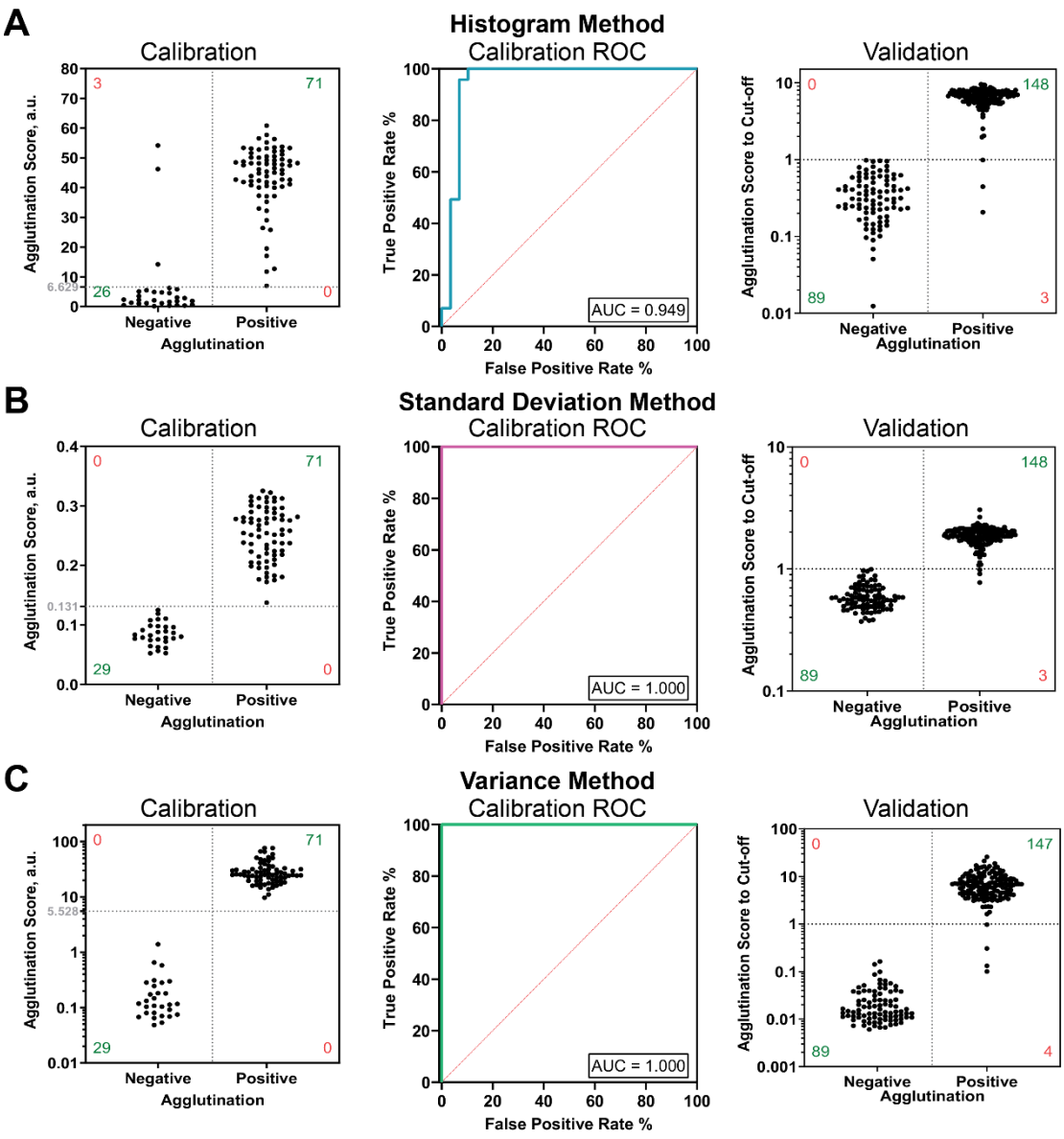

Supplemental Fig. 5. Performance of alternate image analysis algorithms for agglutination assessment.

Plots depicting agglutination assessment performance for alternatives to DAAD, including (A) the histogram method, (B) the standard deviation method, and (C) the variance method. Left: vertical scatter plots of agglutination scores determined by each method for a calibration set of n = 100 ROI images which included 71 agglutinated and 29 non-agglutinated samples. The best-performing thresholds (or cut-offs, shown as gray dashed lines) were determined and used to evaluate the validation set. Middle: receiver operating characteristic (ROC) curves determined from the calibration set (teal, pink, green); the red-dashed lines represent the result of random guesses (coin flip). Right: vertical scatter plots of the ratios of agglutination scores to cut-offs determined by each method for a validation set of n = 240 ROI images which included 151 agglutinated and 89 non-agglutinated samples. The numbers in green and red in the scatter-plots denote the numbers of correct/incorrect assessments for each algorithm.

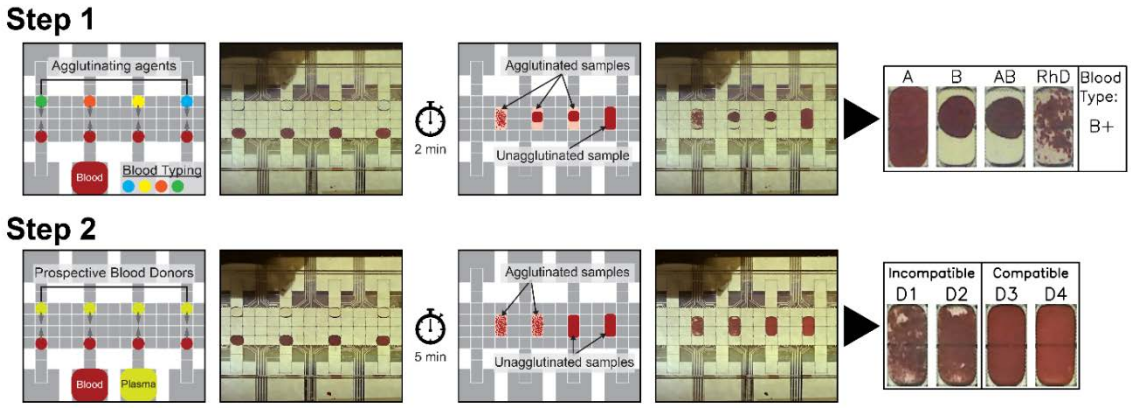

Supplemental Fig. 6. DMF-DAAD for donor compatibility tests.
Cartoons (left columns) and corresponding photographs (right columns) illustrating a proof-of-concept for a donor-recipient crossmatch test on DMF in two steps (each read left-to-right). Step 1 (top) is a standard blood typing assessment to determine the blood type of the recipient's blood, in which four droplets of the recipient's blood are dispensed and mixed with droplets of four blood typing antibodies (cartoon: blue – anti-A, yellow – anti-B, orange – anti-A,B, and green – anti-D) and then analyzed by DAAD. The digital patient card (right) indicates that the recipient's blood type is B+. Step 2 (bottom) is a crossmatching assessment for a potential blood-donor recipient, in which four droplets of the recipient's blood are dispensed and mixed with droplets of plasma from four different potential donors (cartoon: bright yellow) and then analyzed by DAAD. The digital patient card (right) indicates that potential donors 1-2 are not compatible and potential donors 3-4 are compatible with the recipient.

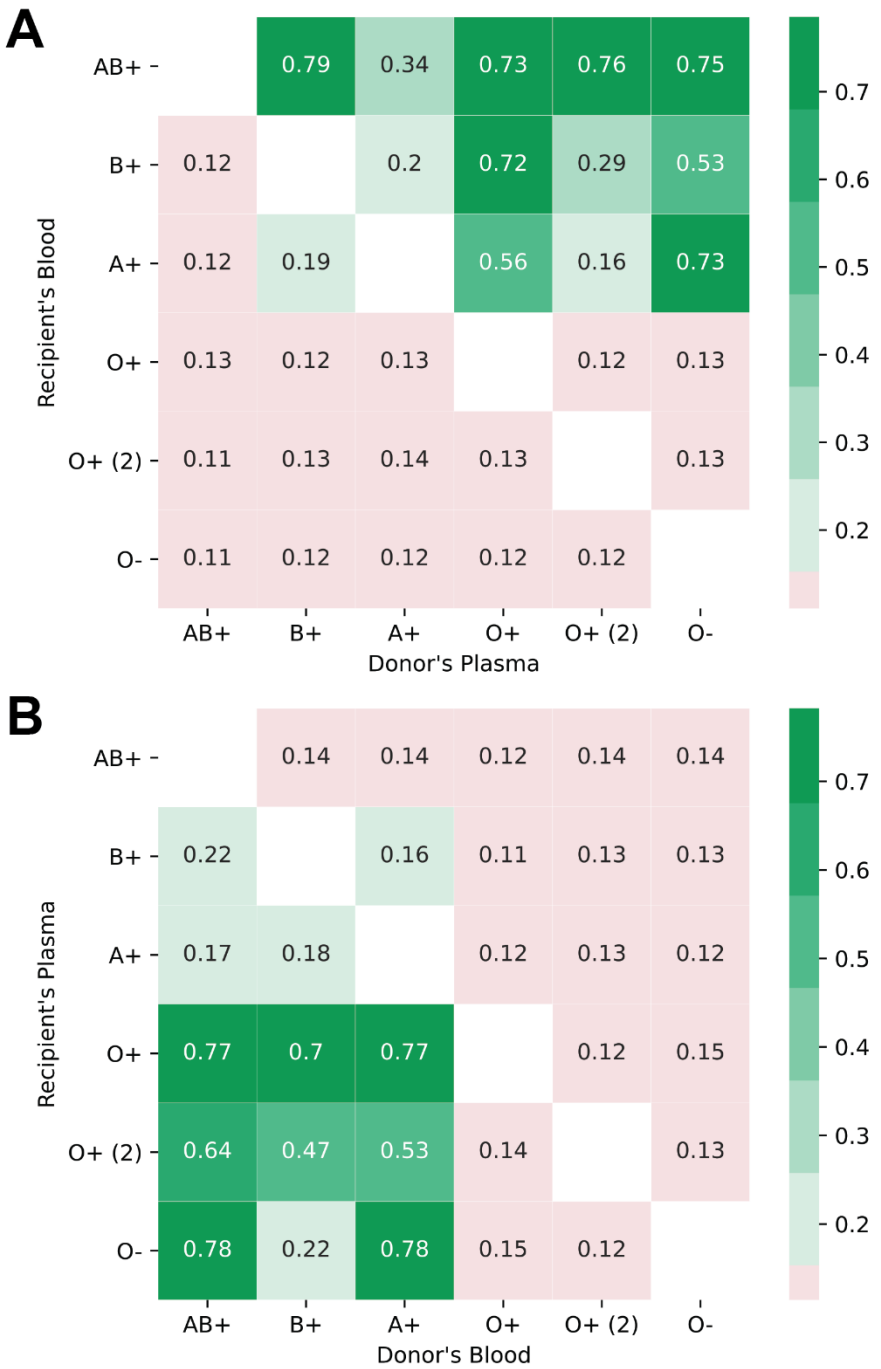

Supplemental Fig. 7. DMF-DAAD donor compatibility matrix.
Six donor blood samples were collected and typed by DMF-DAAD as being AB+, B+, A+, O+, O+ (2), and O-. Each sample was then tested for compatibility relative to the others (also by DMF-DAAD). (A) Heat-map (green-high, red-low) of DMF-DAAD agglutination scores for mock "recipient" whole blood (rows) cross-matched with mock "donor" plasma samples (columns). (B) Heat-map (green-high, red-low) of DMF-DAAD agglutination scores for mock "recipient" plasma (rows) cross-matched with mock "donor" whole blood samples (columns). The patterns are as predicted given the known ABO types. Samples from different RhD groups did agglutinate, indicating that the negative donor hadn't been exposed previously to RhD antigens.

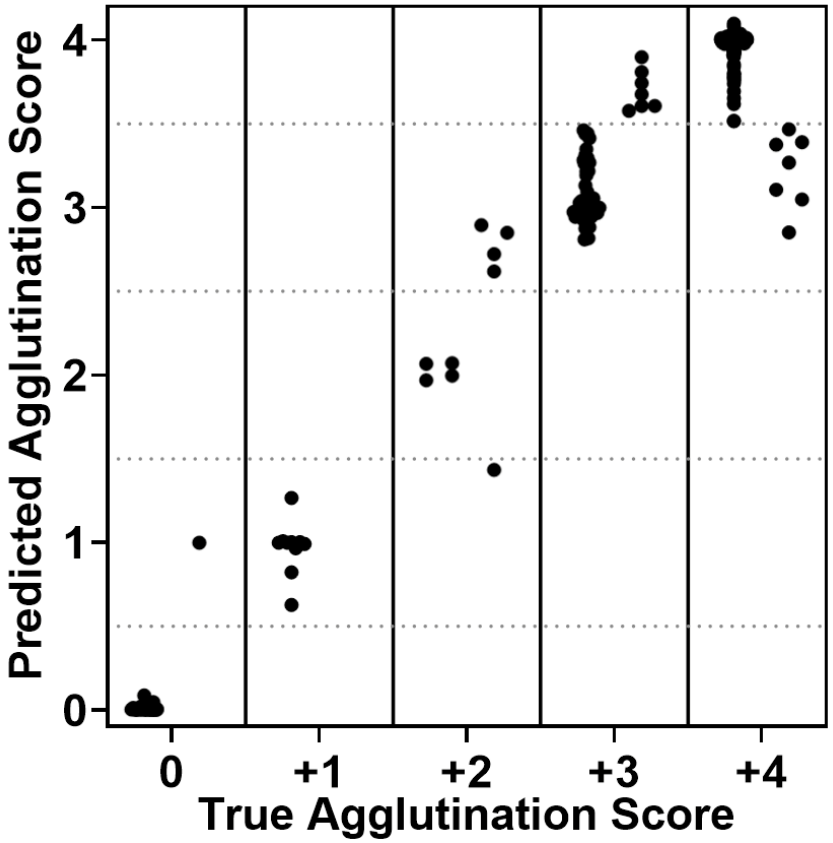

Supplemental Fig. 8. Quantitative agglutination scoring for blood typing.
Data are shown as a scatter plot of predicted agglutination scores grouped by the assigned labels (true agglutination score) for 567 ROI images, under a ten-fold cross-validation procedure. Class thresholds indicated by the dotted gray lines delineate the boundaries between each score; prediction accuracy overall was 97%. For the binary classification (positive vs negative agglutination) only 1 false positive prediction was made out of 567.

Supplemental Movie 1 (separate file). Blood typing assay.
Time-accelerated (4X) movie depicting hemagglutination assay steps for blood typing on a DMF device. The top panel shows different views of the control software while the bottom panel is a live camera feed from the DMF device. Initially, four blood typing antibody solutions (from bottom-left to bottom-right: blue – anti-A, yellow – anti-B, colorless – anti-A,B, colorless – anti-D) are loaded onto the top reservoir electrodes and then unit droplets of each antibody solution are metered and dispensed. Then whole blood is loaded into two reservoirs and four unit droplets are metered and dispensed. Each whole blood droplet is merged with one of the reagent droplets, forming a two-electrode product-droplet. The product droplets are mixed by moving in a rectangular pattern. Agglutination occurs upon reaction of the blood sample with the antibodies. The blood type of the sample used in this movie was A+.

Supplemental Movie 2 (separate file). Parallel operation.
Time accelerated (8x) movie illustrating simultaneous blood typing, donor compatibility testing, and hematocrit measurement. Initially, four blood typing antibody solutions (from top-left to top-right: colorless – Merquat-100, colorless – anti-D, yellow – anti-B and blue – anti-A) are loaded onto the top reservoir electrodes and plasma from a donor is loaded onto a bottom reservoir electrode and then unit droplets of each solution are metered and dispensed. Then whole blood is loaded into two reservoirs and five unit droplets are metered and dispensed. Each whole blood droplet is merged with one of the reagent droplets, forming a two-electrode product-droplet. The product droplets are mixed by moving in a rectangular pattern. Agglutination occurs upon reaction of the blood sample with the antibodies. The blood type of the sample used in this movie was A+, the hematocrit 49%, and the plasma was also from an A+ donor.

Supplemental Movie 3 (separate file). Dried reagents.
Time-accelerated (8X) movie depicting hemagglutination assay steps for blood typing and hematocrit measurement on a DMF device with pre-dried reagents. The device features dried spots [from bottom-left to bottom-right: Merquat-100, anti-D, anti-A,B, anti-B (which includes yellow dye) and anti-A (which includes blue dye)]. Initially, diluent is loaded into the top reservoir electrode and then five unit droplets are metered and dispensed. Each droplet is used to reconstitute one dried reagent, and the reconstituted reagent droplets are moved to the top electrodes. Whole blood is loaded into two reservoirs and five unit droplets are metered and dispensed. Each whole blood droplet is merged with one of the reagent droplets, forming a two-electrode product-droplet. The product droplets are mixed by moving in a rectangular pattern. Agglutination occurs upon reaction of the blood sample with the antibodies or the chemical agglutination agent. The blood type of the sample used in this movie was A+ and the hematocrit 56%.

Supplemental Movie 4 (separate file). Pump operation for automatic refill of a DMF reservoir.
Time-accelerated (10X) movie depicting the auto-pump operation. The left of the frame shows DMF device operations and the right of the frame shows capacitance readings.